

# Luciferase-based reporter system for *in vitro* evaluation of elongation rate and processivity of ribosomes

Ivan Kisly, Carolin Kattel, Jaanus Remme and Tiina Tamm <sup>\*</sup>

Institute of Molecular and Cell Biology, University of Tartu, Tartu 51010, Estonia

Received May 14, 2020; Revised February 09, 2021; Editorial Decision February 10, 2021; Accepted February 12, 2021

## ABSTRACT

The elongation step of translation is a key contributor to the abundance, folding and quality of proteins and to the stability of mRNA. However, control over translation elongation has not been thoroughly investigated. In this study, a Renilla–firefly luciferase fusion reporter system was further developed to investigate the *in vitro* elongation rate and processivity of ribosomes independent of the initiation and termination steps. The reporter mRNA was constructed to contain a single ORF encoding in-frame Renilla luciferase, a specific domain moiety and firefly luciferase. Such a reporter structure enables the quantitative and individual evaluation of the synthesis of a specific domain. As a proof of principle, the synthesis of three protein domains of different lengths and structures was analyzed. Using a cell-free translation assay, both the elongation rate and processivity of ribosomes were shown to vary depending on the domain synthesized. Additionally, a stalling sequence consisting of ten rare arginine codons notably reduced the elongation rate and the processivity of the ribosomes. All these results are consistent with the previously known dynamics of elongation *in vivo*. Overall, the methodology presented in this report provides a framework for studying aspects that contribute to the elongation step of translation.

## INTRODUCTION

Translation of mRNA is a complex energy-consuming process of high importance for the normal physiology of any cell. Translation can be divided into four ordered steps: initiation, elongation, termination and ribosome recycling. Initiation is long known to be a rate-limiting and hence the most vigorously regulated step of translation (1–3). Interestingly, a growing body of evidence suggests the presence of control over elongation, termination and ribosome recycling

as well (2,3). In particular, elongation of translation appears to be extensively regulated by translation factors, translational recoding, secondary structures of mRNA, adaptation of mRNA to the tRNA pool and the charge of a nascent polypeptide chain (2,4–7). As a consequence, regulation of elongation can affect the abundance, folding and quality of synthesized proteins and the stability of mRNA. However, despite recent advances, the mechanisms of control over translation elongation have not been sufficiently studied.

Investigation of the principles of protein synthesis *in vivo* is constrained not only by the complexity of the translational apparatus but also by the complexity and variability of living cells. In light of this, cell-free protein synthesis (CFPS) systems have become attractive alternatives since they offer direct control over the conditions of translation, allowing for the easy optimization of the expression of recombinant proteins. Currently, numerous CFPS platforms have been successfully used in fundamental and applied research: studies of translational machinery, genetic code and gene circuits, metabolic engineering, and production of recombinant proteins, such as antibodies, therapeutic proteins, and virus-like particles (8,9). The most simple, fast and cheap and therefore most often utilized, are uncoupled batch CFPS reactions that contain all necessary components in one tube. These reactions are primed by the addition of an *in vitro* transcribed reporter mRNA encoding a protein of interest. The efficiency of protein synthesis is then estimated by measuring the properties of the produced polypeptides: gel densitometry, amount of fluorescence or incorporated isotope-labelled amino acids, and activity of encoded enzymes (e.g. luciferase, chloramphenicol acetyltransferase or  $\beta$ -galactosidase) (10–15).

Typically, reporters used in CFPS reactions are monocistronic mRNAs encoding a single protein with a specific property. For instance, such reporters have been used to investigate the principles of cap-dependent translation initiation and the influence of codon usage on the rate of translation elongation (7,11,16–18). Alternatively, bicistronic reporters encoding two separate proteins or one fusion protein can be utilized. These reporters have been used to

<sup>\*</sup>To whom correspondence should be addressed. Tel: +372 7375031; Fax: +372 7420286; Email: ttamm@ut.ee

study various aspects of protein synthesis, including IRES-dependent translation initiation, frameshifting, and 'stop-carry on' translational recoding (19–25). As an exception, a tripartite reporter has been introduced in which a single ORF encodes in-frame Renilla luciferase,  $\beta$ -galactosidase and firefly luciferase, which are separated by 2A peptides of the foot-and-mouth disease virus (26). Such a complex reporter has been used to assess the processivity of ribosomes during elongation of translation *in vitro*.

The most commonly utilized reporter proteins for CFPS reactions are firefly luciferase (from *Photinus pyralis*) and Renilla luciferase (from the sea pansy *Rotylenchulus reniformis*). The use of luciferases in CFPS reactions has several advantages: (i) luciferases fold cotranslationally in eukaryotic systems (27,28); (ii) the fusion of luciferases with other polypeptides does not affect their enzymatic activity (26,27,29) and (iii) commercially available assays for bioluminescence measurement provide fast, sensitive (high signal-to-noise ratio) and reliable analysis. All these factors make luciferases a convenient tool for the quantitative characterization of protein synthesis *in vitro*. Recently, a novel mRNA reporter encoding a Renilla–firefly luciferase fusion was employed to evaluate the importance of interactions between ribosomal subunits for the functionality of eukaryotic ribosomes (30). The use of dual luciferases allows for the distinguishing of the initiation and elongation steps of translation, which has shown that the ribosomal intersubunit bridge eB13 is important for translation elongation (30).

In this study, a further development of a dual luciferase reporter system, as reported in a previously published study (30), is presented. As described in this study, the reporters contained a region of interest inserted between the Renilla and firefly luciferase coding regions. This allowed us to assess the elongation rate and the processivity of ribosomes on different mRNA sequences independently of the initiation and termination steps. Moreover, the effect of ribosome stalling on translation elongation was defined.

## MATERIALS AND METHODS

### Plasmids

All plasmids used in this study are listed in the Supplementary Table S1. Construction of the *pUC18-Dual* plasmid was described previously (previous name *pUC18-Rluc-Fluc*) (30). To generate the *pUC18-Dual73*, *pUC18-Dual81* and *pUC18-Dual118* plasmids, the fragments of the *Saccharomyces cerevisiae* *SNF7* gene (166–375 bp from the CDS start), *MLC1* gene (4–237 bp from the CDS start) and *YAH1* gene (172–516 bp from the CDS start), respectively, were amplified by PCR from the genomic DNA. PCR products were cloned into the *SalI* restriction site of the *pUC18-Dual* plasmid.

The *pUC18-Dual146* plasmid, containing tandem repeat of two *SNF7* gene fragments, was generated in two steps. First, the fragment of the *S. cerevisiae* *SNF7* gene (166–375 bp from the CDS start) was amplified by PCR from the genomic DNA, cut by *XhoI* and *SalI* restriction enzymes, and cloned into the *SalI* restriction site of the *pUC18-Dual* plasmid. Next, the same fragment of the *SNF7* gene was amplified by PCR from the genomic DNA, cut by *SalI* restriction

enzyme only, and cloned into the *SalI* restriction site of the plasmid generated in the first step.

To generate the *pUC18-DualR10* plasmid, the forward primer encoding for the R10 sequence (5' CGG CGA CGA CGG CGC CGC CGG CGA CGA CGG 3') and the reverse primer encoding for the 5' end of the firefly luciferase CDS were annealed and extended by PCR. Obtained PCR fragments were used to substitute the general spacer and the 5' end of the firefly luciferase CDS between the *SalI* and *XbaI* restriction sites of the *pUC18-Dual* plasmid.

### Preparation of extracts for yeast cell-free translation

Yeast cell-free translation extracts were prepared as described previously using *S. cerevisiae* strain TYSC309 (*MATa ura3–52 leu2 $\Delta$ 1 his3 $\Delta$ 200 trp1 $\Delta$ 36  $\Delta$ arg4  $\Delta$ lys1*) (30,31). Yeast cells were grown in 1 l of YPD (1% bacto yeast extract, 2% bacto peptone, 2% glucose) at 30°C until OD<sub>600</sub> of 1.9–2.0. The cells were collected by centrifugation (10 min, 2404 × g, 4°C), washed (5 min, 2404 × g, 4°C) four times (one time with 20 ml followed by three times with 10 ml) with ice-cold mannitol buffer A [30 mM HEPES–KOH pH 7.5, 100 mM KOAc, 3 mM Mg(OAc)<sub>2</sub>, 8.5% mannitol (w/v), 2 mM DTT]. This yielded in ~3 g of cell pellet that was immediately resuspended in the ice-cold mannitol buffer A supplemented with 0.5 mM PMSF (1.5 ml of buffer per 1 g of cells). The cells were disrupted by glass beads ( $\varnothing$  0.25–0.5 mm; ~500  $\mu$ l of beads per 900  $\mu$ l of cells) in 2 ml tubes in the Precellys 24 homogenizer (Bertin Technologies) (program: 6000 rpm, 3 × 60 s, pause 60 s, 4°C). Lysates were divided between two TLA 100.3 tubes (Beckman Coulter) and clarified by ultracentrifugation for 6 min at 30 000 × g, 4°C. Supernatants were transferred into a new TLA 100.3 tubes and additionally clarified for 10 min at 30 000 × g, 4°C. Next, 2 ml of clarified extract was loaded onto the hand-made 20 ml gel filtration column [Econo-Pac<sup>®</sup> Disposable Chromatography Column (Bio-Rad) packed with the Sephadex G-25 Fine matrix (GE Healthcare Life Sciences)] equilibrated with buffer A [30 mM HEPES–KOH pH 7.5, 100 mM KOAc, 3 mM Mg(OAc)<sub>2</sub>, 2 mM DTT, 0.5 mM PMSF]. The extract was passed through the column at a flow rate of 0.5 ml/min and 200  $\mu$ l fractions were collected. Fractions with *A*<sub>260</sub> higher than 75% of a maximal *A*<sub>260</sub> were pooled. This yielded 1200  $\mu$ l of extract with concentration of 120–130 *A*<sub>260</sub> absorbance units per ml of extract. Next, CaCl<sub>2</sub> was added to a final concentration of 0.5 mM and the obtained extract was treated with the micrococcal nuclease (Thermo Scientific) at a final concentration of 0.18 U/ $\mu$ l for 10 min at 25°C. The reaction was stopped by the addition of EGTA (pH 8.0) to a final concentration of 2 mM. The nuclease treated extract was aliquoted by 20 and 50  $\mu$ l, frozen in liquid N<sub>2</sub> and stored at –80°C.

### mRNA synthesis

All plasmids were linearized by the *BamHI* to generate a linear template for *in vitro* transcription reaction. mRNA was synthesized for 2 h at 42°C in 50  $\mu$ l reactions containing 1  $\mu$ g of linear DNA, 3.75 mM of each rNTP, 50 mM NH<sub>4</sub>Cl, 200 mM HEPES–KOH pH 7.5, 30 mM MgCl<sub>2</sub>, 30 mM DTT, 2 mM spermidine, 40 U RiboLock RNase Inhibitor (Thermo Scientific) and 250 U of a home-made T7

RNA polymerase. Next, the reaction mixtures were treated with 10 U of DNaseI (VWR Life Science AMRESCO) for 20 min at 37°C. The mRNA was purified by acidic phenol-chloroform, precipitated by ethanol and capped using Vaccinia Capping System (New England Biolabs) according to the manufacturer protocol. The capped mRNA was purified by the RNeasy Mini Kit (QIAGEN GmbH) in accordance with the user manual, aliquoted, frozen in liquid N<sub>2</sub> and stored at -80°C. The integrity of mRNA was confirmed by agarose gel electrophoresis.

### ***In vitro* translation**

Fifteen microliters of translation mixture [44 mM HEPES-KOH (pH 7.5), 240 mM KOAc, 4 mM Mg(OAc)<sub>2</sub>, 1.5 mM ATP, 0.2 mM GTP, 3.4 mM DTT, amino acid mix (0.08 mM of each), 50 mM creatine phosphate (Sigma-Aldrich), 500 ng mRNA, 0.4 μg/μl creatine phosphokinase (Sigma-Aldrich), 60 U RiboLock RNase Inhibitor (Thermo Scientific) and 15 μl of yeast nuclease treated extract were separately preincubated for 5 min at 25°C. Next, the extract was added to the translation mixture (1:1 ratio) to a final volume of 30 μl and incubated at 25°C. At the indicated time points, 2 μl reaction samples were frozen in liquid N<sub>2</sub>. The reaction samples were thawed on ice immediately before the luciferase activity measurement. Firefly and Renilla luciferase activities were measured by the Dual-Luciferase<sup>®</sup> Reporter Assay System (Promega) by adding 50 μl of LARII followed by adding 50 μl of Stop&Glo reagent. All measurements were performed using a Tecan Infinite M200 Pro plate reader (Tecan Group Ltd.) in 96-well microplates [F-bottom/chimney well, LUMITRAC<sup>™</sup> 600 med. binding (Greiner Bio-One)] using an integration time of 10 s. At least four independent reactions and two independent mRNA batches were analyzed for each mRNA reporter.

To radioactively label the translation products, methionine in the translation mixture was substituted with 1 μl of EasyTag<sup>™</sup> methionine L-[<sup>35</sup>S] (10.25 mCi/ml stock, Perkin Elmer). Reactions were carried out in a 30 μl final volume for 80 min at 25°C, and terminated by adding standard SDS-PAGE sample buffer. Samples were denatured for 5 min at 95°C and analyzed in 10% SDS-PAGE. Gels were fixed in a 50% ethanol-10% acetic acid solution for 40 min, dried and exposed to a Storage Phosphor Screen (FUJIFILM) for 17 h. Screens were analyzed by the Amersham<sup>™</sup> Typhoon<sup>™</sup> RGB Biomolecular Imager (GE Healthcare Life Sciences).

### **Data analysis**

To determine the time of the first appearance (TFA) of the luminescence signal of the Renilla and firefly luciferases, the activities of luciferases in *in vitro* translation reactions were monitored over 11 min and relative light units were plotted against the time points. The mean background luminescence was determined and the upper limit for the background luminescence was calculated as the mean + 4 SD. The TFA value was defined as the point of intercept between the regression line and the upper limit of background luminescence. Next, ΔTFA values were calculated as TFA<sub>Fluc</sub> - TFA<sub>Rluc</sub>. The time needed to translate additional coding re-

gions or the R10 sequence (T<sub>add</sub>) was calculated with the following equation:

$$T_{\text{add}} = \Delta\text{TFA}_{\text{Mod}} - \Delta\text{TFA}_{\text{Dual}}$$

where ΔTFA<sub>Mod</sub> is a ΔTFA value for the Dual73, Dual81, Dual118, Dual146 or DualR10 reporters and ΔTFA<sub>Dual</sub> is a ΔTFA value for the Dual reporter. The rate of elongation was defined by the following equation:

$$v_{\text{elong}} = \frac{T_{\text{add}}}{N}$$

where *N* is the number of codons in the added coding region or R10 sequence.

Renilla and firefly luciferase activity curves were determined by monitoring the activities of luciferases over 80 min of the *in vitro* translation reactions. Slopes for a linear part of the obtained activity curves between 20 and 40 min were determined, and ratios between slope<sub>Fluc</sub> and slope<sub>Rluc</sub> values were calculated. The overall processivity on the additional coding regions or apparent processivity on an R10 sequence (*P*<sub>general</sub>) was calculated with the following equation:

$$P_{\text{general}} = \frac{\text{Ratio}_{\text{Mod}}}{\text{Ratio}_{\text{Dual}}}$$

where Ratio<sub>Mod</sub> is a slope ratio for Dual73, Dual81, Dual118, Dual146 or DualR10 reporters, and Ratio<sub>Dual</sub> is a slope ratio for dual reporter. Processivity of the ribosomes at each codon was calculated with the following equation:

$$P_{\text{codon}} = \sqrt[N]{P_{\text{general}}}$$

where *N* is the number of codons in an added coding region or R10 sequence. Consequently, the loss of processivity was determined as 1 - *P*<sub>codon</sub>.

Relative codon adaptiveness was calculated using the Graphical Codon Usage Analyzer 2.0 (32). The Codon Adaptation Index was calculated using CAIcal (33) and Codon Usage Database (34). The tRNA Adaptation Index (tAI) was calculated as described previously (35) using tAI for each codon as described in a previously published report (36). The normalized tRNA Adaptation Index (ntAI) was calculated according to a previously published report (37). The minimal folding energy (MFE) for mRNA sequences in 40-nt windows was calculated using the ViennaRNA package (38) as described in a previously published report (5). The molecular weights (Mw) and theoretical isoelectric points (pI) of the polypeptides were calculated using the Expasy server (39). Statistical significance of differences was analyzed by ANOVA and a *post hoc* Bonferroni test at a significance level of 0.05. Protein structures were generated by PyMOL (40) using coordinates from previously published reports (41-43).

## **RESULTS AND DISCUSSION**

### **Principle of *in vitro* synthesis of the Renilla-firefly luciferase fusion**

It has been previously shown that the reporter mRNA encoding the Renilla-firefly luciferase fusion can be used to



compare the initiation efficiency, processivity and elongation rates of mutant and wild-type ribosomes during translation *in vitro* (30). This reporter, designated as 'Dual' here, contains a cap structure, a 45-nt *PGK1* 5'-UTR, a single ORF encoding Renilla luciferase (311 codons), a general spacer (13 codons) and firefly luciferase (552 codons), followed by a 14-nt 3'-UTR and a 30-nt poly(A) tail (Figures 1 and 2). Cotranslational folding of Renilla and firefly luciferases enables the precise definition of translational parameters, such as the time needed to synthesize each luciferase moiety (Figure 1A). The luminescence signal of Renilla luciferase becomes detectable when ribosomes complete synthesis of the Renilla luciferase moiety of the fusion protein. Therefore, the time of the first appearance of the luminescence signal of Renilla luciferase ( $TFA_{Rluc}$ ) reflects the time needed for the initiation of translation and synthesis of the Renilla luciferase moiety (Figure 1B). Since Renilla and firefly luciferases are encoded by the same ORF, the ribosomes that have synthesized the Renilla luciferase moiety continue translation and eventually synthesize the general spacer and firefly luciferase moiety of the fusion protein (Figure 1A). Firefly luciferase has been shown to become active immediately upon release from the ribosome (28). Thus, the time of the first appearance of the luminescence signal of firefly luciferase ( $TFA_{Fluc}$ ) reflects the time needed for one round of translation consisting of initiation, elongation and termination steps (Figure 1B). Consequently, the difference between the  $TFA_{Fluc}$  and  $TFA_{Rluc}$  values ( $\Delta TFA$ ) represents the time needed to synthesize the general spacer and firefly luciferase moiety and terminate translation (Figure 1B).

The activities of both the Renilla and firefly luciferases showed a sigmoid curve during *in vitro* translation reactions (Figure 1C). The slope of the linear part of the Renilla luciferase activity time course ( $slope_{Rluc}$ ) depends on the number of ribosomes that initiate translation and complete the synthesis of the Renilla luciferase moiety. In turn, the slope of the linear part of the firefly luciferase activity time course ( $slope_{Fluc}$ ) depends on the number of ribosomes that complete synthesis of the whole fusion protein. The ratio between the  $slope_{Fluc}$  and  $slope_{Rluc}$  values reflects the processivity, i.e. the probability of the ribosomes completing the synthesis of the whole protein after completion of the Renilla luciferase moiety (Figure 1C).

To assess the rate of elongation, a system of reporters was introduced, where additional coding regions of different lengths were inserted between the Renilla and firefly luciferase coding sequences (Figure 2 and Supplementary Figure S1). The additional regions encoded protein domains with experimentally determined 3D structures. These domains were expected not to interfere with the folding or activity of either luciferase. The additional coding region in the Dual73 reporter contained a fragment of the *S. cerevisiae* *SNF7* coding sequence, which was inserted into the general spacer. This region encodes a 73 amino acid residue-long  $\alpha$ -helical domain (41). Similarly, the inserted region in the Dual81 reporter contained a fragment of the *MLC1* coding sequence and encoded the 81 amino acid-long globular domain consisting of short helices (42). The additional region in the Dual118 reporter contained a fragment of the *YAH1* coding sequence and encoded the 118 amino acid-

long globular  $\alpha/\beta$  domain (43). In the Dual146 reporter, the additional coding region contained a tandem repeat of two *SNF7* coding sequence fragments. As a result, this region encoded two 73 amino acid-long  $\alpha$ -helical domains. All reporters (Dual, Dual73, Dual81, Dual118 and Dual146) had the same 5'- and 3'-UTRs, so initiation and termination of translation was expected to occur on these reporters at the same rate.

#### Analysis of the elongation rate and processivity of ribosomes *in vitro*

To determine the elongation rate of ribosomes, the activities of Renilla and firefly luciferases over 11 min of translation were monitored, and TFA values were determined for each reporter (Figures 3A, B and 4A, B, Table 1).  $TFA_{Rluc}$  values for all reporters were identical within error limits, indicating three important aspects: (i) a similar rate of initiation; (ii) a similar activity of Renilla luciferase, despite fusion with additional domains and (iii) a similar quality of transcribed mRNA. This was also supported by the similarities between the Renilla luciferase activity curves of all reporters (Figures 3A, C and 4A, C). For each reporter, the time needed to complete the synthesis of the whole protein after synthesis of the Renilla luciferase moiety ( $\Delta TFA$ ) was calculated (Table 1). In the case of reporters with inserted sequences, the ribosomes needed extra time to translate these sequences, which led to increased  $\Delta TFA$  values compared to the Dual reporter (Figure 3A, B and Table 1). In the case of the Dual146 reporter, the increase in the  $\Delta TFA$  value was proportional to the length of the second *SNF7* fragment compared to the Dual73 reporter (Figure 4A, B and Table 1). Consequently, the time needed to translate each additional coding region ( $T_{add}$ ) was calculated as the difference between  $\Delta TFA$  values for reporters with and without such a region. Knowing the length of the added regions and the time needed to translate each region, the average rate of elongation ( $v_{elong}$ ) on each added region was calculated (Table 1). The highest rate of elongation was detected for the 81 amino acid-long globular domain encoded by the Dual81 reporter (2.58 aa/s) (Table 1). This rate of elongation is similar to an average elongation rate of 2.63 aa/sec, which has been recently reported for *S. cerevisiae* ORFs (44). As a comparison, the ribosomes exhibited a 1.3 times lower rate of elongation during the synthesis of the 73 amino acid-long  $\alpha$ -helical domain encoded by the Dual73 reporter. Moreover, the rate of elongation during the synthesis of this domain was similar for the Dual73 and Dual146 reporters (Table 1). The slowest rate of elongation was detected for ribosomes synthesizing the 118 amino acid-long globular domain encoded by the Dual118 reporter (Table 1). Altogether, these data indicate that the rate of elongation varies depending on the added coding region. Indeed, the rate of elongation has been recently shown to vary up to 20-fold among yeast ORFs (44).

The rate of elongation is influenced by codon usage bias, availability of cognate tRNAs, structure of mRNA and charge of the translated protein (5–7,45). All additional coding regions analyzed here exhibited similar codon adaptation and tRNA adaptation indexes (Supplementary Table S2). To analyze possible mRNA secondary structures, pro-

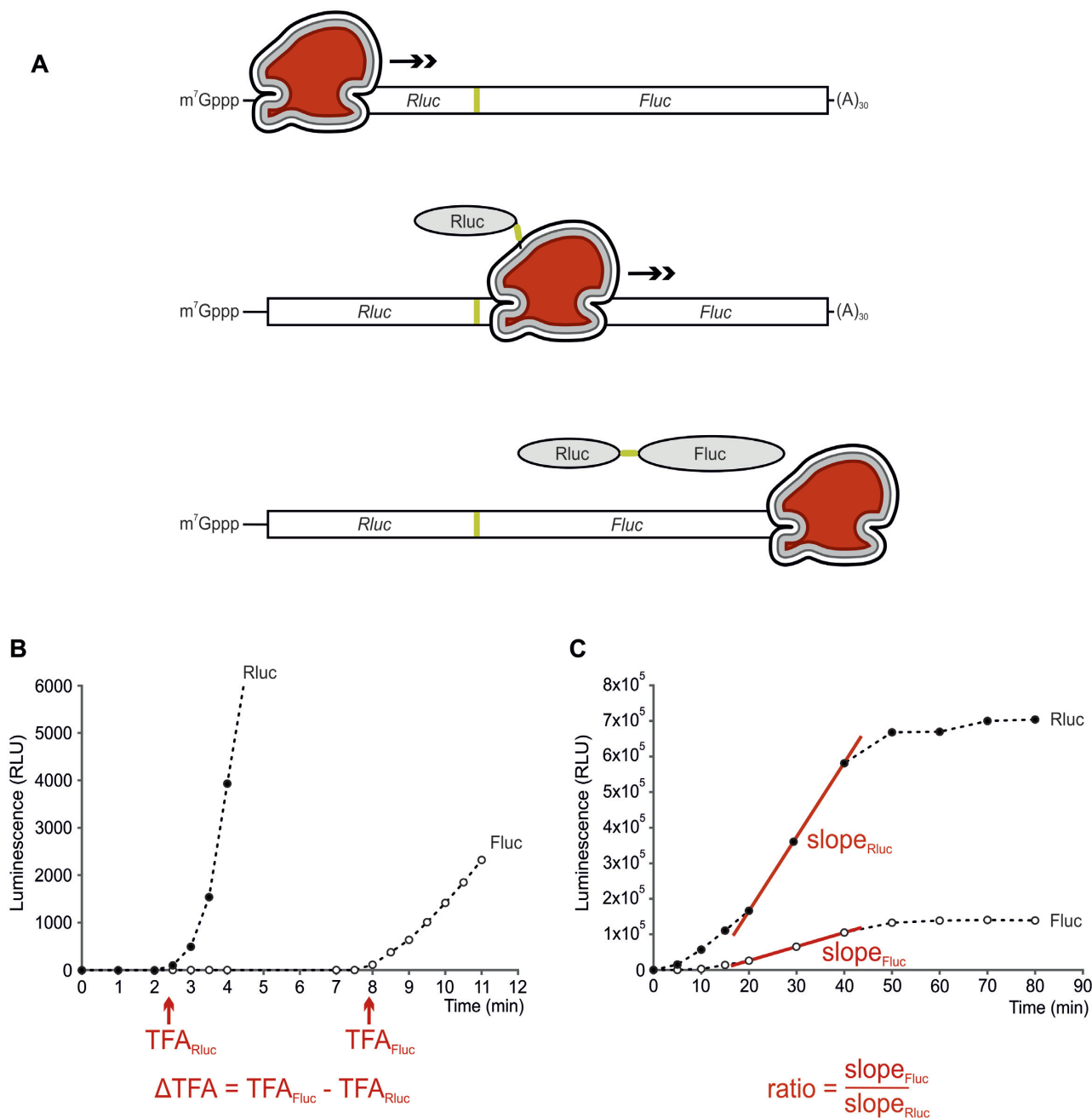


**Figure 1.** Principle of *in vitro* synthesis of the Renilla–firefly luciferase fusion. (A) Schematic representation of the cotranslational folding of the Renilla and firefly luciferase moieties of the fusion protein. The luminescence signal from the measurement of Renilla luciferase activity becomes detectable when the Renilla luciferase moiety is synthesized. The luminescence signal from the measurement of firefly luciferase activity becomes detectable when a whole fusion protein is synthesized. Positions of the general spacer (gold), m<sup>7</sup>Gppp cap structure and poly(A)<sub>30</sub> tail are indicated. (B) Schematic representation of the time of the first appearance of the luminescence signal from the Renilla (TFA<sub>Rluc</sub>) and firefly (TFA<sub>Fluc</sub>) luciferase activity measurements. TFA<sub>Rluc</sub> combines the time needed for initiation of translation and synthesis of the Renilla luciferase moiety. TFA<sub>Fluc</sub> reflects the time needed for one round of translation.  $\Delta TFA$  depends on the time needed to complete the synthesis of the firefly luciferase moiety and terminate translation. (C) Schematic representation of the Renilla and firefly luciferase activity time course over 80 min of *in vitro* translation. The slope of the linear part of the Renilla luciferase activity curve (slope<sub>Rluc</sub>) depends on the number of ribosomes that initiated translation and completed synthesis of the Renilla luciferase moiety. The slope of the linear part of the firefly luciferase activity curve (slope<sub>Fluc</sub>) depends on the number of ribosomes that complete the synthesis of the whole protein. The ratio between the slope<sub>Fluc</sub> and slope<sub>Rluc</sub> values reflects the processivity of ribosomes.

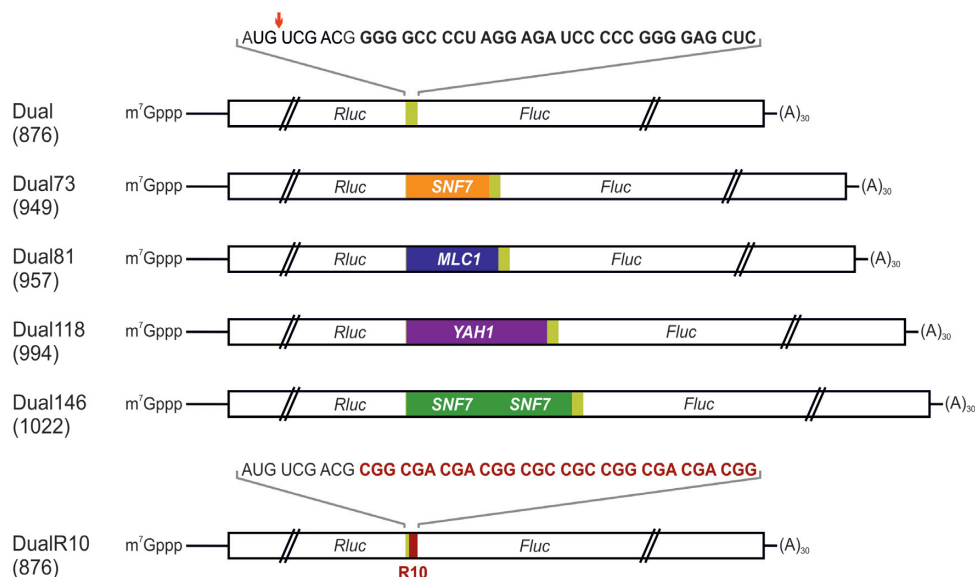


**Figure 2.** mRNA reporters used in this study. Schematic representation of the Dual, Dual73, Dual81, Dual118, Dual146 and DualR10 reporters. Lengths of the ORFs in codons are shown in brackets. Positions of the m<sup>7</sup>Gppp cap structure and poly(A)<sub>30</sub> tail are indicated. The general spacer is shown in gold. In the Dual reporter, the red arrow indicates the insertion point for additional coding regions. Bold letters indicate the sequence substituted for the R10 stalling sequence in the DualR10 reporter. Additional coding regions for the Dual73, Dual81, Dual118 and Dual146 reporters are coloured orange, blue, purple and green, respectively. For the DualR10 reporter, the position and sequence of the R10 stalling sequence is shown in bold red.

files of local minimal folding energies (MFE) corresponding to sliding windows of 40 nucleotides were computed for the Dual73, Dual81 and Dual118 reporters (Supplementary Figure S2). Such energy profiles have been previously used to characterize the stability of mRNA secondary structures that have to be unfolded in front of the elongating ribosome (5). The lowest MFE value (−20.6 kcal/mol) was revealed at the start of the firefly luciferase coding region and was the same for all reporters. In the case of inserted sequences, all MFE values were higher than −17 kcal/mol. Thus, the observed variations in the elongation rate are probably not due to stable stem-loop structures in the mRNAs analyzed. However, the formation of more complex higher-order mRNA structures cannot be excluded. In the future, the reporter system described here will allow us to extensively analyze the effect of mRNA secondary structure on the rate of translation elongation. Analysis of the charge of translated proteins demonstrated a high theoretical *pI* (9.35) for the  $\alpha$ -helical domain moiety of Snf7 encoded by the Dual73 reporter (Supplementary Table S2). It has been shown that the *pI* of proteins negatively correlates with the rate of elongation (44). Therefore, the high positive charge of this domain moiety might explain the decreased rate of elongation compared to the Dual81 reporter (Table 1 and Supplementary Table S2). In the case of the Dual118 reporter, the domain moiety of Yah1 demonstrated a low theoretical *pI*, similar to that of the Dual81 reporter (Supplementary Table S2). However, this domain moiety had the most complex structure, containing a combination of  $\alpha$ -helices and  $\beta$ -sheets folded into the globule (Supplementary Figure S1C). It is tempting to speculate that the slow elongation rate might allow optimal cotranslational folding of the Yah1 domain moiety (Table 1) (37,46,47). The detailed mechanism of how the charge of a nascent polypeptide and

the structure of a synthesized protein contribute to the dynamics of translation elongation must be revealed in future studies. Altogether, these results demonstrate that the described reporter system can be used to specifically assess the elongation rate of ribosomes on different ORFs and to study aspects that contribute to this process.

To determine the processivity of ribosomes, the time course of luciferase activities was monitored over 80 min, and the slope values were determined (Figures 3C, D and 4C, D, Table 2). No statistically significant difference between slope<sub>Rluc</sub> values was detected for all tested reporters, which again indicates a similar rate of initiation on these reporters (Table 2). Calculations of the firefly and Renilla luciferase activity slope ratios demonstrated decreased ratios for the reporters with inserted sequences compared to the Dual reporter (Table 2). Importantly, in the case of the Dual146 reporter, the insertion of the second *SNF7* fragment led to proportionally decreased slope ratio values compared to the Dual73 reporter (Figure 4C, D and Table 2). These results indicate that the ribosomes lose processivity during the translation of an additional coding region, which results in a decreased number of ribosomes successfully translating the firefly luciferase coding sequence. Each ribosome can be simply described as a molecular motor that moves codon by codon along the mRNA molecule, and at each codon one amino acid residue is added to the polypeptide chain. Thus, the decreased slope ratios for reporters with additional coding regions reflect the reduced probability of the ribosomes continuing their movement after *N* codons of the respective region. This is defined as an overall processivity of ribosomes on each additional region ( $P_{\text{general}}$ ) (Table 2). Consequently, the average processivity of the ribosome at each codon of an additional region ( $P_{\text{codon}}$ ) and the average probability of the ribosome aborting trans-

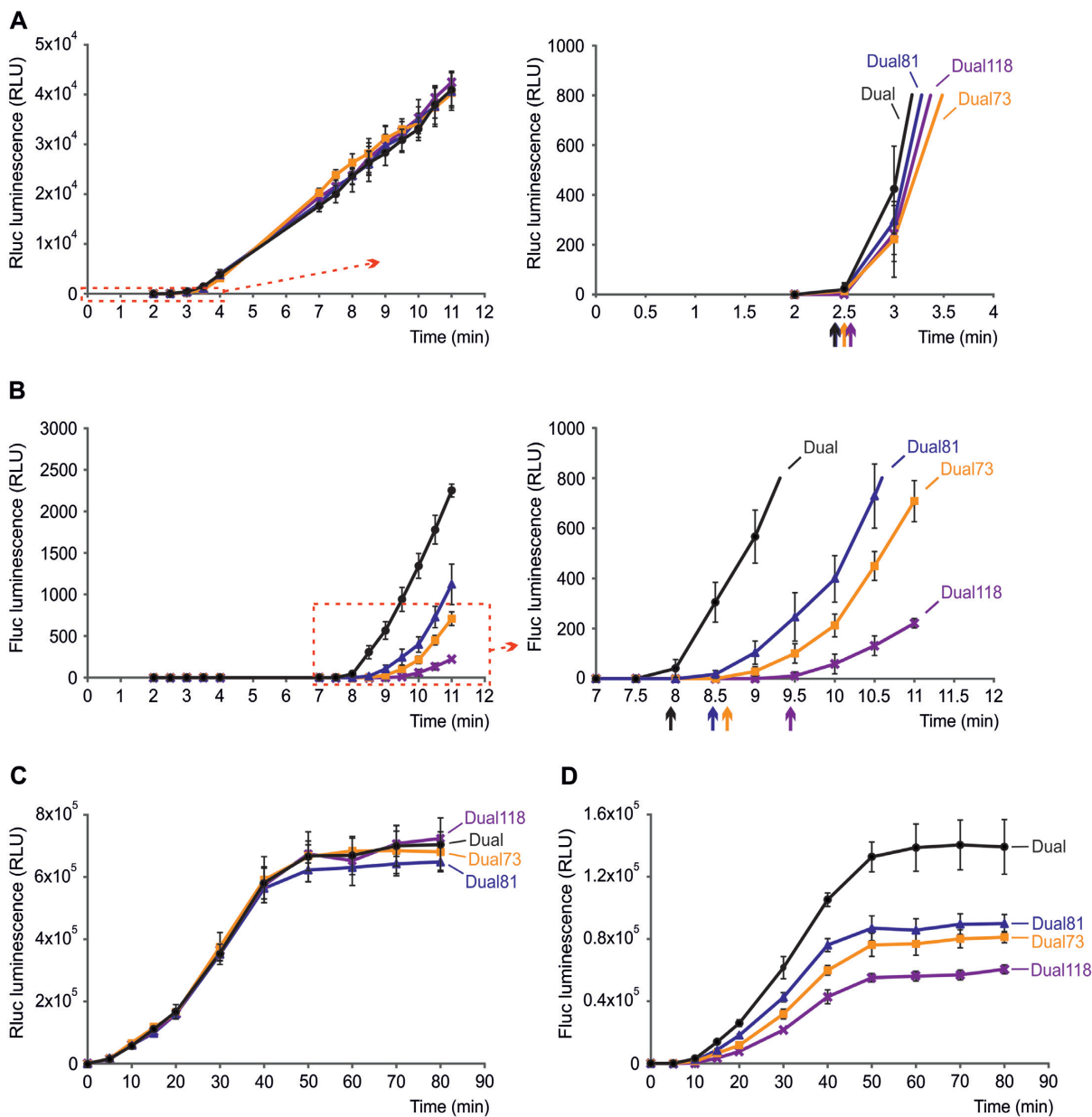


**Figure 3.** Analysis of the Renilla and firefly luciferase activities in reactions primed with the Dual, Dual73, Dual81 and Dual118 reporters. The time of the first appearance of the luminescence signal (TFA) from the Renilla (A) and firefly (B) luciferase activity measurements during the 11 min of *in vitro* translation is shown. The area under the red dashed-line rectangle is magnified and displayed on the right. TFAs are indicated by arrows. Time courses of Renilla (C) and firefly (D) luciferase activities over 80 min of *in vitro* translation are shown. All reactions were carried out at 25°C in a 30  $\mu$ l starting volume using 500 ng of reporter mRNA as a template, and the activities of both luciferases were measured in the same reaction. For each reporter, two independent mRNA batches were analyzed, and each batch was analyzed by at least two independent reactions. The average (mean  $\pm$  SD) relative light units (RLU) of all reactions are plotted. No statistically significant difference in Renilla luciferase activities (panels A and C) was revealed between reporters by the ANOVA and *post hoc* Bonferroni test at a significance level of 0.05.

lation at each codon (loss of processivity) can be calculated. Ribosomes conferred a similar probability of losing processivity while translating the additional regions of the Dual73 and Dual118 reporters. Moreover, the loss of ribosome processivity was similar on the additional coding regions of the Dual73 and Dual146 reporters, both encoding the Snf7 domain (Table 2). In contrast, ribosomes had an  $\sim$ 2 times lower probability of aborting translation on the additional region of the Dual81 reporter (Table 2). This indicates that

not only the rate of elongation but also the processivity of the ribosomes varies among the coding sequences.

The current model of translation elongation suggests that not all ribosomes complete translation of the ORF after initiation of translation (26,48–51). Ribosome profiling (Ribo-Seq) data indicate that the density of ribosomes decreases slowly along the mRNA due to a spontaneous ribosome drop-off (49). Drop-off was also shown in an *in vitro* system with a tripartite mRNA reporter encoding in-frame Re-

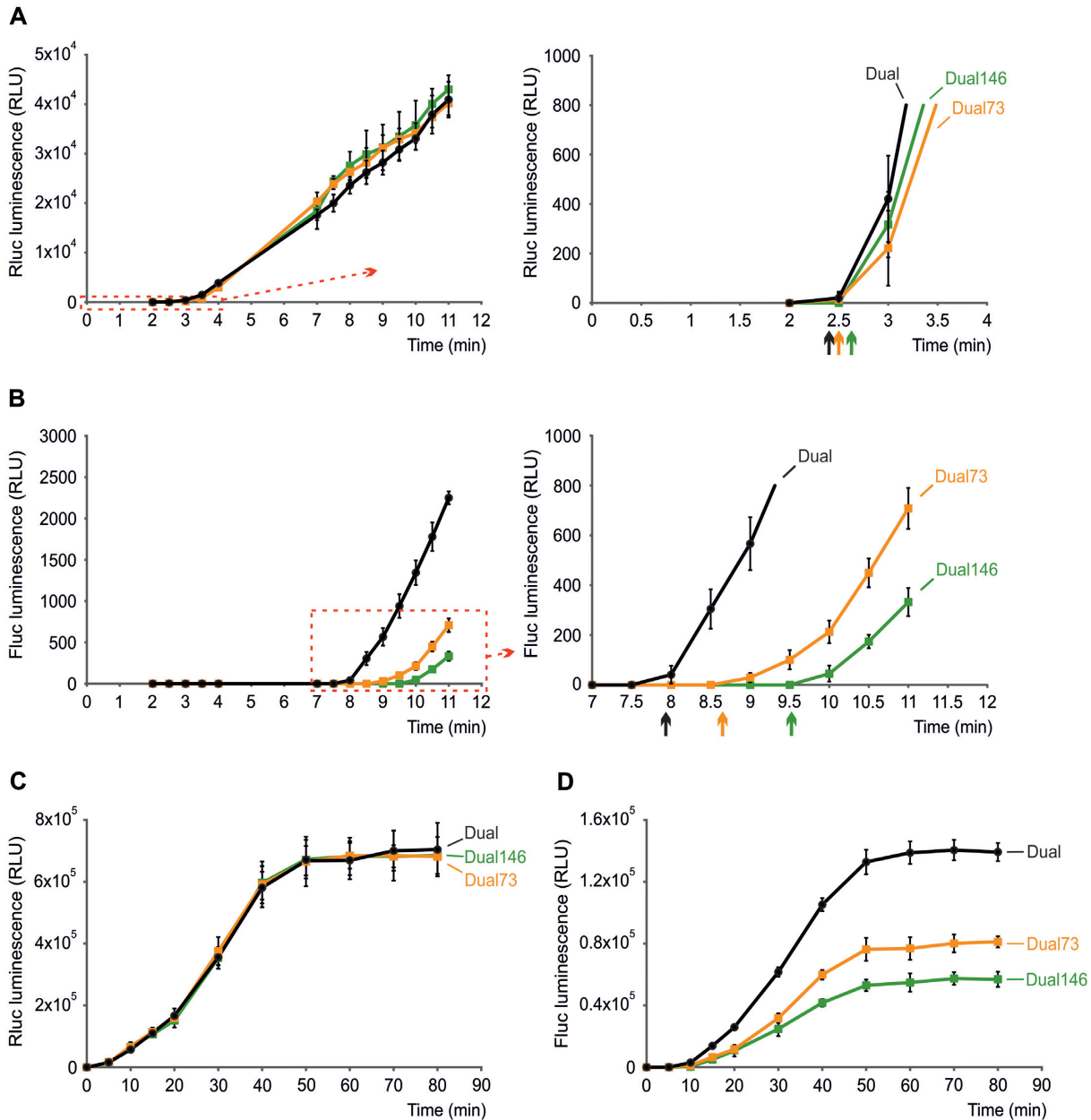


**Figure 4.** Analysis of the Renilla and firefly luciferase activities in reactions primed with the Dual, Dual73 and Dual146 reporters. The time of the first appearance of the luminescence signal (TFA) from the Renilla (A) and firefly (B) luciferase activity measurements during the 11 min of *in vitro* translation is shown. The area under the red dashed-line rectangle is magnified and displayed on the right. TFAs are indicated by arrows. Time courses of Renilla (C) and firefly (D) luciferase activities over 80 min of *in vitro* translation are shown. All reactions were carried out at 25°C in a 30  $\mu$ l starting volume using 500 ng of reporter mRNA as a template, and the activities of both luciferases were measured in the same reaction. For each reporter, two independent mRNA batches were analyzed, and each batch was analyzed by at least two independent reactions. The average (mean  $\pm$  SD) relative light units (RLU) of all reactions are plotted. No statistically significant difference in Renilla luciferase activities (panels A and C) was revealed between reporters by the ANOVA and *post hoc* Bonferroni test at a significance level of 0.05.

nilla luciferase,  $\beta$ -galactosidase, and firefly luciferase (26). Analysis revealed that only 32% of ribosomes reached the end of the firefly luciferase ORF after synthesis of Renilla luciferase (26). Several studies computationally predicted the processivity of eukaryotic ribosomes to be in the range of 99.44–99.99% per elongation step (48–50). This study conferred similar processivity of ribosomes ranging from 99.27% to 99.64% per elongation step. Therefore, the re-

porter system described here allows us to assess the processivity of ribosomes on different ORFs.

#### Effect of stalling on the translation elongation

The above findings demonstrate that the translation rate and processivity depend on the nature of the coding sequences. It has been shown that the elongation step of trans-



**Table 1.** Analysis of elongation rate of ribosomes (related to Figures 3A–B, 4A–B and 5A–B)

Reporter	Dual	Dual73	Dual81	Dual118	Dual146	DualR10
<sup>a</sup> <i>N</i> (codons)	–	73	81	118	146	–
<sup>b</sup> TFA <sub>Rluc</sub> (min)	2.40 ± 0.12	2.50 ± 0.18	2.41 ± 0.12	2.57 ± 0.07	2.63 ± 0.09	2.45 ± 0.04
<sup>c</sup> TFA <sub>Fluc</sub> (min)	<sup>1</sup> 7.94 ± 0.05	<sup>2</sup> 8.65 ± 0.12	<sup>2</sup> 8.47 ± 0.11	<sup>3</sup> 9.45 ± 0.20	<sup>3,4</sup> 9.52 ± 0.02	<sup>4</sup> 9.82 ± 0.16
<sup>d</sup> ΔTFA (min)	5.54 ± 0.11	6.15 ± 0.10	6.06 ± 0.09	6.87 ± 0.20	6.89 ± 0.08	7.37 ± 0.16
<sup>e</sup> <i>T</i> <sub>add</sub> (s)	–	36.30 ± 8.75	31.40 ± 8.29	80.04 ± 13.79	81.00 ± 8.20	109.65 ± 11.77
<sup>f</sup> <i>v</i> <sub>elong</sub> (aa/s)	–	<sup>1,2</sup> 2.01 ± 0.48	<sup>2</sup> 2.58 ± 0.68	<sup>1</sup> 1.47 ± 0.25	<sup>1</sup> 1.80 ± 0.18	<sup>3</sup> 0.09 ± 0.01

For each parameter, the average (mean ± SD) of 4–6 reactions is shown.

<sup>a</sup>Length of the additional domain inserted between the Renilla and firefly luciferase moieties.

<sup>b</sup>Time of the first appearance of the luminescence signal of Renilla luciferase. No statistically significant difference between the TFA<sub>Rluc</sub> values was revealed by ANOVA and *post hoc* Bonferroni tests at a significance level of 0.05.

<sup>c</sup>Time of the first appearance of the luminescence signal of firefly luciferase. Numbers (1–4) indicate statistically homogeneous groups according to ANOVA and *post hoc* Bonferroni tests at a significance level of 0.05. The same numbers denote no statistically significant difference.

<sup>d</sup>Difference between the TFA<sub>Fluc</sub> and TFA<sub>Rluc</sub> values.

<sup>e</sup>Time needed to synthesize an additional coding region or R10 stalling sequence.

<sup>f</sup>Rate of elongation. Numbers (1–3) indicate statistically homogeneous groups according to ANOVA and *post hoc* Bonferroni tests at a significance level of 0.05.

**Table 2.** Analysis of processivity of ribosomes (related to Figures 3C–D, 4C–D and 5C–D)

Reporter	Dual	Dual73	Dual81	Dual118	Dual146	DualR10
<sup>a</sup> <i>N</i> (codons)	–	73	81	118	146	–
<sup>b</sup> Slope <sub>Rluc</sub> (x10 <sup>3</sup> ; RLU/min)	20.73 ± 2.43	21.5 ± 3.60	20.22 ± 1.60	20.80 ± 2.81	22.26 ± 2.75	21.18 ± 2.73
<sup>c</sup> Slope <sub>Fluc</sub> (x10 <sup>3</sup> ; RLU/min)	<sup>1</sup> 3.97 ± 0.25	<sup>2</sup> 2.41 ± 0.19	<sup>2,3</sup> 2.90 ± 0.19	<sup>4</sup> 1.76 ± 0.21	<sup>4</sup> 1.55 ± 0.27	<sup>3</sup> 3.34 ± 0.39
<sup>d</sup> Slope ratio	0.19 ± 0.02	0.11 ± 0.02	0.14 ± 0.01	0.08 ± 0.01	0.07 ± 0.02	0.16 ± 0.01
<sup>e</sup> <i>P</i> <sub>general</sub>	–	0.59 ± 0.11	0.75 ± 0.02	0.44 ± 0.05	0.37 ± 0.09	0.82 ± 0.05
<sup>f</sup> <i>P</i> <sub>codon</sub> (x10 <sup>-2</sup> )	–	99.27 ± 0.23	99.64 ± 0.03	99.31 ± 0.09	99.30 ± 0.16	98.05 ± 0.65
<sup>g</sup> 1 – <i>P</i> <sub>codon</sub> (x10 <sup>-2</sup> )	–	<sup>2</sup> 0.73	<sup>1</sup> 0.36	<sup>2</sup> 0.69	<sup>2</sup> 0.70	<sup>3</sup> 1.95

For each parameter, the average (mean ± SD) of 4–5 reactions is shown.

<sup>a</sup>Length of the additional domain inserted between the Renilla and firefly luciferase moieties.

<sup>b</sup>Slope of the linear part of the Renilla luciferase activity time course. No statistically significant difference between TFA<sub>Rluc</sub> values was revealed by ANOVA and *post hoc* Bonferroni tests at a significance level of 0.05.

<sup>c</sup>Slope of the linear part of the firefly luciferase activity time course. Numbers (1–4) indicate statistically homogeneous groups according to ANOVA and *post hoc* Bonferroni tests at a significance level of 0.05. The same numbers denote no statistically significant difference.

<sup>d</sup>Ratio between the slope<sub>Fluc</sub> and slope<sub>Rluc</sub> values.

<sup>e</sup>Processivity of ribosomes on the additional coding region or apparent processivity on the R10 sequence.

<sup>f</sup>Processivity of ribosomes per codon.

<sup>g</sup>Loss of processivity per codon. Numbers (1–3) indicate statistically homogeneous groups according to ANOVA and *post hoc* Bonferroni tests at a significance level of 0.05. The same numbers denote no statistically significant difference.

lation can be affected by rare codons and positively charged amino acids that cause ribosome stalling (5–7,45). To analyze the effect of stalling on translation elongation using this luciferase system, a DualR10 reporter was introduced. In this reporter, ten codons of the general spacer between the Renilla and firefly luciferase moieties were substituted by the R10 stalling sequence consisting of ten rare arginine codons (Figure 2 and Supplementary Figure S3, Supplementary Table S2). This stalling sequence has been shown to cause ribosome pausing *in vitro* and *in vivo* (52–55).

The elongation rate of ribosomes on the R10 sequence was determined as described above. The TFA<sub>Rluc</sub> and TFA<sub>Fluc</sub> values were measured for the DualR10 reporter, and ΔTFA was calculated (Figure 5A, B and Table 1). No statistically significant difference between TFA<sub>Rluc</sub> values for the Dual and DualR10 reporters was detected, showing that the R10 sequence did not affect the synthesis of the Renilla luciferase moiety. However, since ribosomes on the DualR10 reporter needed additional time to move along the stalling sequence, the delay of the TFA<sub>Fluc</sub> and increase of the ΔTFA value were detected. Ribosomes needed an addi-

tional ~109 s to translate the R10 sequence compared to the general spacer of the Dual reporter (Table 1). Therefore, the R10 sequence dramatically reduces the rate of elongation.

To analyze the effect of stalling on the processivity of ribosomes, slope values were determined for the DualR10 reporter, and the slope ratio was calculated (Figure 5C, D and Table 2). The decreased slope ratio in the case of the DualR10 reporter corresponds to a decreased apparent processivity (*P*<sub>general</sub>) of ribosomes on the R10 coding sequence compared to the general spacer of the Dual reporter (Table 2). As a result, ribosomes had a ~1.95% chance of losing processivity at each arginine codon of the R10 sequence. Analysis of the [<sup>35</sup>S]methionine-labelled translation products by SDS-PAGE showed strong accumulation of intermediate products caused by the stalling of ribosomes at the R10 sequence (Supplementary Figure S4). These data show that the stalling of ribosomes leads to an increased probability of ribosomes dissociating from mRNA.

Altogether, the use of the described reporter system allows us to quantitatively analyze the effect of ribosome pausing on the elongation step of translation. These re-

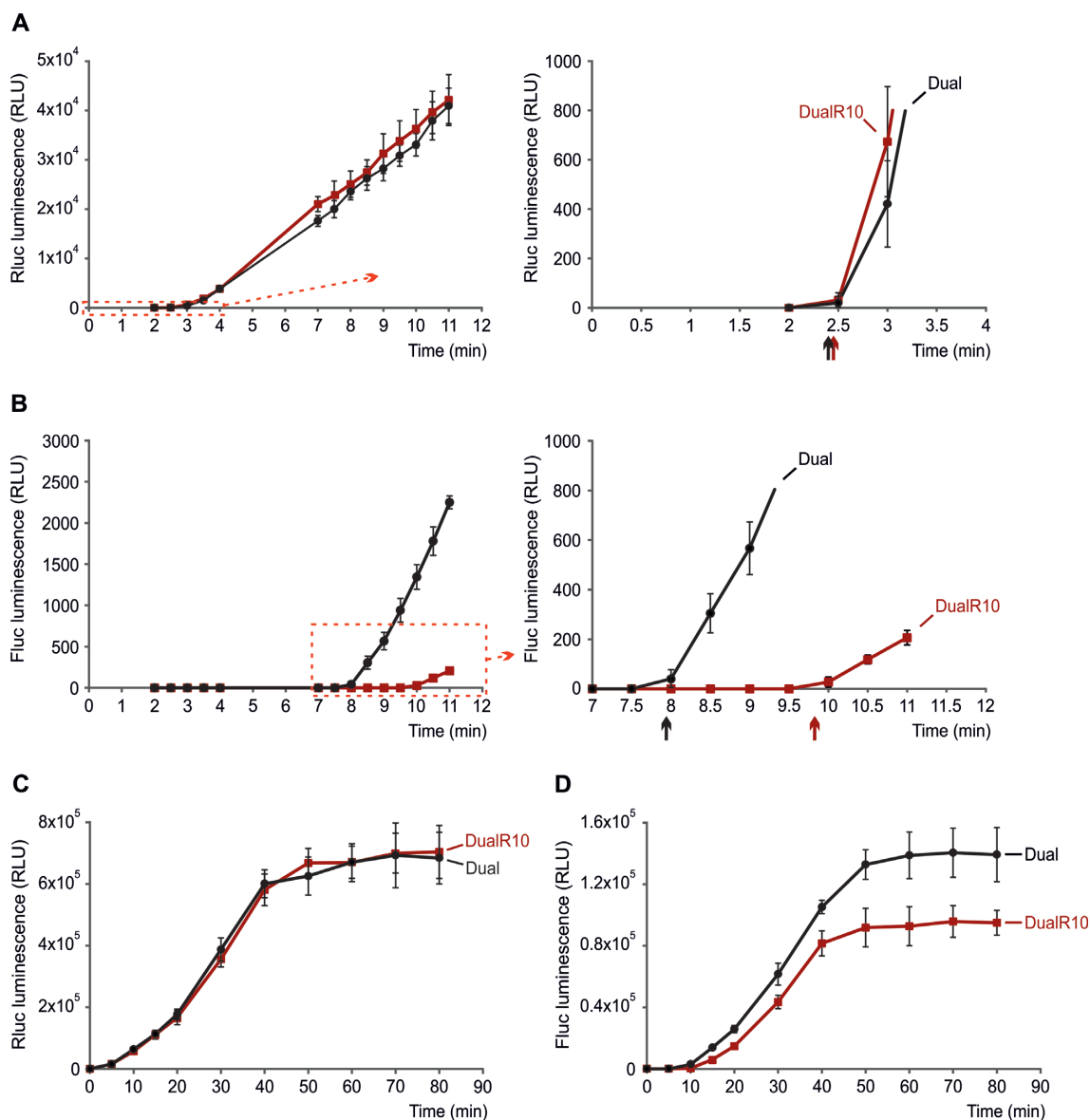


**Figure 5.** Analysis of the Renilla and firefly luciferase activities in reactions primed with the Dual and DualR10 reporters. The time of the first appearance of the luminescence signal (TFA) from the Renilla (A) and firefly (B) luciferase activity measurements during the 11 min of *in vitro* translation is shown. The area under the red dashed-line rectangle is magnified and displayed on the right. TFAs are indicated by arrows. Time courses of the Renilla (C) and firefly (D) luciferase activities over 80 min of *in vitro* translation are shown. All reactions were carried out at 25°C in a 30  $\mu$ l starting volume using 500 ng of reporter mRNA as a template, and the activities of both luciferases were measured in the same reaction. For each reporter, two independent mRNA batches were analyzed, and each batch was analyzed by at least two independent reactions. The average (mean  $\pm$  SD) relative light units (RLU) of all reactions are plotted. No statistically significant difference in Renilla luciferase activities (panels A and C) was revealed between reporters by the unpaired *t*-test at a significance level of 0.05.

sults demonstrate that the rate of elongation decreases when ribosomes translate ten rare codons encoding positively charged amino acid residues, which is consistent with published studies (52,54,56). Moreover, the stalling of ribosomes leads to reduced processivity.

## CONCLUSION

In this study, a system of multipartite mRNA reporters for *in vitro* analysis of translation elongation was described. Each reporter contains a single ORF encoding a fusion pro-

tein, which consists of a Renilla luciferase moiety, sequence of interest and firefly luciferase moiety. Synthesis of the Renilla luciferase moiety serves as a control of the initiation rate and reflects the quality of the mRNA reporter. Synthesis of the firefly luciferase moiety depends on the elongation events occurring during the translation of an upstream-located sequence of interest. Therefore, the described system makes it possible to compare translation elongation on different coding regions independent of initiation and termination steps. Elongation in this system can be characterized by several parameters. First, the time of the first ap-

pearance (TFA) of the luminescence signal can be determined for each luciferase. Analysis of differences between the Renilla and firefly luciferase TFA values allows us to estimate the rate of elongation on the studied coding sequences. Second, processivity can be defined as a ratio between slopes of linear parts of the firefly and Renilla luciferase activity curves. The use of slope ratios allows us to assess the overall processivity of ribosomes on the coding sequence of interest and the average processivity at each codon. Finally, since the final product is synthesized as a fusion protein, intermediate translation products can be easily tracked back to specific reporter regions by SDS-PAGE or other methods.

The reporter system described in this study has several advantages:

- **Simplicity.** All key experimental components are commercially available, and the system is easily reproducible in a general molecular biology laboratory.
- **Universality.** This system allows for the direct determination of both the rates of elongation and processivity of ribosomes on any coding sequence of interest. Moreover, since initiation is a rate-limiting step of translation, the slope of the Renilla luciferase activity curve can be used to assess the initiation of translation.
- **Portability.** The principle behind this system can be used in any eukaryotic cell-free translation system analogous to the one described here. This approach can also be further adapted to allow continuous luminescence monitoring for high-throughput studies. In addition, the development of a similar system to study translation elongation in cell-free extracts of animal cells would be of great benefit.

However, one should bear in mind the high variability of elongation rates determined by this reporter system, which is the result of the delicacy of cell-free translation reactions, relatively short lengths of the analyzed domains and the high rate of translation. The coding sequence inserted between the Renilla and firefly luciferase sequences should be carefully designed to allow the elongation rate to be distinctively evaluated. Estimation of elongation rates also depends on the accuracy of the TFA value measurements. In addition, it must be pointed out that the processivity of ribosomes varies on different codons. Therefore, the processivity calculated here reflects the average processivity of the ribosome at each codon of an analyzed sequence.

The system described here can be used to analyze the translation pausing caused by different factors that include mRNA secondary structure. In this regard, extensive mutational and bioinformatical analysis of mRNA structures along with optimization of *in vitro* RNA folding must be carried out.

The results of this study suggest that this reporter system, based on a Renilla–firefly luciferase fusion, is a reliable and inexpensive tool for the direct analysis of ribosome elongation rate and processivity on different mRNA sequences. This system is attractive to a variety of studies, such as investigation of the correlation between elongation rate and protein folding, mutational analysis of translational machinery and screening for novel translation-inhibiting compounds.

## SUPPLEMENTARY DATA

Supplementary Data are available at NAR Online.

## ACKNOWLEDGEMENTS

We thank all members of the Chair of Molecular Biology, especially Dr Aivar Liiv and Dr Margus Leppik for advice and support, and Silva Lilleorg, Kaspar Reier, Ermo Leuska, Vlad-Julian Piljukov and Natalja Garber for fruitful discussions. We are grateful to Maie Loorits for technical assistance.

## FUNDING

Estonian Research Council [PUT PRG669, PRG1179 to J.R.]. Funding for open access charge: Estonian Research Council.

*Conflict of interest statement.* None declared.

## REFERENCES

1. Shah, P., Ding, Y., Niemczyk, M., Kudla, G. and Plotkin, J.B. (2013) Rate-limiting steps in yeast protein translation. *Cell*, **153**, 1589–1601.
2. Dever, T.E., Kinzy, T.G. and Pavitt, G.D. (2016) Mechanism and regulation of protein synthesis in *Saccharomyces cerevisiae*. *Genetics*, **203**, 65–107.
3. Sokabe, M. and Fraser, C.S. (2019) Toward a kinetic understanding of Eukaryotic translation. *Cold Spring Harb. Perspect. Biol.*, **11**, a032706.
4. Dever, T.E., Dinman, J.D. and Green, R. (2018) Translation elongation and recoding in Eukaryotes. *Cold Spring Harb. Perspect. Biol.*, **10**, a032649.
5. Tuller, T., Veksler-Lublinsky, I., Gazit, N., Kupiec, M., Rupp, E. and Ziv-Ukelson, M. (2011) Composite effects of gene determinants on the translation speed and density of ribosomes. *Genome Biol.*, **12**, R110.
6. Dao Duc, K. and Song, Y.S. (2018) The impact of ribosomal interference, codon usage, and exit tunnel interactions on translation elongation rate variation. *PLoS Genet.*, **14**, e1007166.
7. Yu, C.H., Dang, Y., Zhou, Z., Wu, C., Zhao, F., Sachs, M.S. and Liu, Y. (2015) Codon usage influences the local rate of translation elongation to regulate Co-translational protein folding. *Mol. Cell*, **59**, 744–754.
8. Gregorio, N.E., Levine, M.Z. and Oza, J.P. (2019) A user's guide to cell-free protein synthesis. *Methods Protoc.*, **2**, 24.
9. Khambhati, K., Bhattacharjee, G., Gohil, N., Braddick, D., Kulkarni, V. and Singh, V. (2019) Exploring the potential of Cell-Free protein synthesis for extending the abilities of biological systems. *Front. Bioeng. Biotechnol.*, **7**, 248.
10. Sissons, C.H. (1974) Yeast protein synthesis. Preparation and analysis of a highly active cell-free system. *Biochem. J.*, **144**, 131–140.
11. Tarun, S.Z. Jr, Wells, S.E., Deardorff, J.A. and Sachs, A.B. (1997) Translation initiation factor eIF4G mediates in vitro poly(A) tail-dependent translation. *PNAS*, **94**, 9046–9051.
12. Iizuka, N., Najita, L., Franzusoff, A. and Sarnow, P. (1994) Cap-dependent and cap-independent translation by internal initiation of mRNAs in cell extracts prepared from *Saccharomyces cerevisiae*. *Mol. Cell Biol.*, **14**, 7322–7330.
13. Nomura, Y., Tanaka, H., Poellinger, L., Higashino, F. and Kinjo, M. (2001) Monitoring of in vitro and in vivo translation of green fluorescent protein and its fusion proteins by fluorescence correlation spectroscopy. *Cytometry*, **44**, 1–6.
14. Zubay, G., Lederman, M. and DeVries, J.K. (1967) DNA-directed peptide synthesis. 3. Repression of beta-galactosidase synthesis and inhibition of repressor by inducer in a cell-free system. *PNAS*, **58**, 1669–1675.
15. Iskakov, M.B., Szaflarski, W., Dreyfus, M., Remme, J. and Nierhaus, K.H. (2006) Troubleshooting coupled in vitro transcription-translation system derived from *Escherichia coli* cells: synthesis of high-yield fully active proteins. *Nucleic Acids Res.*, **34**, e135.

16. Tarun, S.Z. Jr and Sachs, A.B. (1995) A common function for mRNA 5' and 3' ends in translation initiation in yeast. *Genes Dev.*, **9**, 2997–3007.
17. Neff, C.L. and Sachs, A.B. (1999) Eukaryotic translation initiation factors 4G and 4A from *Saccharomyces cerevisiae* interact physically and functionally. *Mol. Cell Biol.*, **19**, 5557–5564.
18. Preiss, T., Muckenthaler, M. and Hentze, M.W. (1998) Poly(A)-tail-promoted translation in yeast: implications for translational control. *RNA*, **4**, 1321–1331.
19. Jan, E. and Sarnow, P. (2002) Factorless ribosome assembly on the internal ribosome entry site of cricket paralysis virus. *J. Mol. Biol.*, **324**, 889–902.
20. Costantino, D.A., Pflingsten, J.S., Rambo, R.P. and Kieft, J.S. (2008) tRNA-mRNA mimicry drives translation initiation from a viral IRES. *Nat. Struct. Mol. Biol.*, **15**, 57–64.
21. Brasey, A., Lopez-Lastra, M., Ohlmann, T., Beerens, N., Berkhout, B., Darlix, J.L. and Sonenberg, N. (2003) The leader of human immunodeficiency virus type 1 genomic RNA harbors an internal ribosome entry segment that is active during the G2/M phase of the cell cycle. *J. Virol.*, **77**, 3939–3949.
22. Sharma, P., Yan, F., Doronina, V.A., Escuin-Ordinas, H., Ryan, M.D. and Brown, J.D. (2012) 2A peptides provide distinct solutions to driving stop-carry on translational recoding. *Nucleic Acids Res.*, **40**, 3143–3151.
23. Doronina, V.A., Wu, C., de Felipe, P., Sachs, M.S., Ryan, M.D. and Brown, J.D. (2008) Site-specific release of nascent chains from ribosomes at a sense codon. *Mol. Cell Biol.*, **28**, 4227–4239.
24. Donnelly, M.L.L., Luke, G., Mehrotra, A., Li, X., Hughes, L.E., Gani, D. and Ryan, M.D. (2001) Analysis of the aphthovirus 2A/2B glycoprotein 'cleavage' mechanism indicates not a proteolytic reaction, but a novel translational effect: a putative ribosomal 'skip'. *J. Gen. Virol.*, **82**, 1013–1025.
25. Lucchesi, J., Makelainen, K., Merits, A., Tamm, T. and Makinen, K. (2000) Regulation of -1 ribosomal frameshifting directed by cocksfoot mottle sobemovirus genome. *Eur. J. Biochem.*, **267**, 3523–3529.
26. Bonderoff, J.M. and Lloyd, R.E. (2010) Time-dependent increase in ribosome processivity. *Nucleic Acids Res.*, **38**, 7054–7067.
27. Hillebrecht, J.R. and Chong, S. (2008) A comparative study of protein synthesis in *in vitro* systems: from the prokaryotic reconstituted to the eukaryotic extract-based. *BMC Biotech.*, **8**, 58.
28. Kolb, V.A., Makeyev, E.V. and Spirin, A.S. (1994) Folding of firefly luciferase during translation in a cell-free system. *EMBO J.*, **13**, 3631–3637.
29. Byrd, M.P., Zamora, M. and Lloyd, R.E. (2005) Translation of eukaryotic translation initiation factor 4GI (eIF4GI) proceeds from multiple mRNAs containing a novel cap-dependent internal ribosome entry site (IRES) that is active during poliovirus infection. *J. Biol. Chem.*, **280**, 18610–18622.
30. Kisly, I., Remme, J. and Tamm, T. (2019) Ribosomal protein eL24, involved in two intersubunit bridges, stimulates translation initiation and elongation. *Nucleic Acids Res.*, **47**, 406–420.
31. Tamm, T., Kisly, I. and Remme, J. (2019) Functional interactions of ribosomal intersubunit bridges in *Saccharomyces cerevisiae*. *Genetics*, **213**, 1329–1339.
32. Fuhrmann, M., Hausherr, A., Ferbitz, L., Schodl, T., Heitzer, M. and Hegemann, P. (2004) Monitoring dynamic expression of nuclear genes in *Chlamydomonas reinhardtii* by using a synthetic luciferase reporter gene. *Plant Mol. Biol.*, **55**, 869–881.
33. Puigbo, P., Bravo, I.G. and Garcia-Vallve, S. (2008) CAIcal: a combined set of tools to assess codon usage adaptation. *Biol. Direct*, **3**, 38.
34. Nakamura, Y., Gojobori, T. and Ikemura, T. (2000) Codon usage tabulated from international DNA sequence databases: status for the year 2000. *Nucleic Acids Res.*, **28**, 292.
35. dos Reis, M., Savva, R. and Wernisch, L. (2004) Solving the riddle of codon usage preferences: a test for translational selection. *Nucleic Acids Res.*, **32**, 5036–5044.
36. Tuller, T., Carmi, A., Vestsigian, K., Navon, S., Dorfan, Y., Zaborske, J., Pan, T., Dahan, O., Furman, I. and Pilpel, Y. (2010) An evolutionarily conserved mechanism for controlling the efficiency of protein translation. *Cell*, **141**, 344–354.
37. Pechmann, S. and Frydman, J. (2013) Evolutionary conservation of codon optimality reveals hidden signatures of cotranslational folding. *Nat. Struct. Mol. Biol.*, **20**, 237–243.
38. Lorenz, R., Bernhart, S.H., Honer Zu Siederdisen, C., Tafer, H., Flamm, C., Stadler, P.F. and Hofacker, I.L. (2011) ViennaRNA Package 2.0. *Algorithms Mol. Biol.: AMB*, **6**, 26.
39. Gasteiger, E., Gattiker, A., Hoogland, C., Ivanyi, I., Appel, R.D. and Bairoch, A. (2003) ExPASy: the proteomics server for in-depth protein knowledge and analysis. *Nucleic Acids Res.*, **31**, 3784–3788.
40. Schrodinger, LLC. (2015) The PyMOL Molecular Graphics System, Version 1.5.0.5.
41. Tang, S., Henne, W.M., Borbat, P.P., Buchkovich, N.J., Freed, J.H., Mao, Y., Fromme, J.C. and Emr, S.D. (2015) Structural basis for activation, assembly and membrane binding of ESCRT-III Snf7 filaments. *eLife*, **4**, e12548.
42. Pennestri, M., Melino, S., Contessa, G.M., Casavola, E.C., Paci, M., Ragnini-Wilson, A. and Cicero, D.O. (2007) Structural basis for the interaction of the myosin light chain Mlc1p with the myosin V Myo2p IQ motifs. *J. Biol. Chem.*, **282**, 667–679.
43. Webert, H., Freibert, S.A., Gallo, A., Heidenreich, T., Linne, U., Amlacher, S., Hurt, E., Muhlenhoff, U., Banci, L. and Lill, R. (2014) Functional reconstitution of mitochondrial Fe/S cluster synthesis on Isu1 reveals the involvement of ferredoxin. *Nat. Commun.*, **5**, 5013.
44. Riba, A., Di Nanni, N., Mittal, N., Arhne, E., Schmidt, A. and Zavolan, M. (2019) Protein synthesis rates and ribosome occupancies reveal determinants of translation elongation rates. *PNAS*, **116**, 15023–15032.
45. Charneski, C.A. and Hurst, L.D. (2013) Positively charged residues are the major determinants of ribosomal velocity. *PLoS Biol.*, **11**, e1001508.
46. Zhang, G., Hubalewska, M. and Ignatova, Z. (2009) Transient ribosomal attenuation coordinates protein synthesis and co-translational folding. *Nat. Struct. Mol. Biol.*, **16**, 274–280.
47. Komar, A.A. (2009) A pause for thought along the co-translational folding pathway. *Trends Biochem. Sci.*, **34**, 16–24.
48. Arava, Y., Wang, Y., Storey, J.D., Liu, C.L., Brown, P.O. and Herschlag, D. (2003) Genome-wide analysis of mRNA translation profiles in *Saccharomyces cerevisiae*. *PNAS*, **100**, 3889–3894.
49. Zupanic, A., Meplan, C., Grellscheid, S.N., Mathers, J.C., Kirkwood, T.B., Hesketh, J.E. and Shanley, D.P. (2014) Detecting translational regulation by change point analysis of ribosome profiling data sets. *RNA*, **20**, 1507–1518.
50. Arava, Y., Boas, F.E., Brown, P.O. and Herschlag, D. (2005) Dissecting eukaryotic translation and its control by ribosome density mapping. *Nucleic Acids Res.*, **33**, 2421–2432.
51. Kurland, C.G. (1992) Translational accuracy and the fitness of bacteria. *Annu. Rev. Genet.*, **26**, 29–50.
52. Gamble, C.E., Brule, C.E., Dean, K.M., Fields, S. and Grayhack, E.J. (2016) Adjacent codons act in concert to modulate translation efficiency in Yeast. *Cell*, **166**, 679–690.
53. Ikeuchi, K., Tesina, P., Matsuo, Y., Sugiyama, T., Cheng, J., Saeki, Y., Tanaka, K., Becker, T., Beckmann, R. and Inada, T. (2019) Collided ribosomes form a unique structural interface to induce Hel2-driven quality control pathways. *EMBO J.*, **38**, e100276.
54. Matsuo, Y., Ikeuchi, K., Saeki, Y., Iwasaki, S., Schmidt, C., Udagawa, T., Sato, F., Tsuchiya, H., Becker, T., Tanaka, K. *et al.* (2017) Ubiquitination of stalled ribosome triggers ribosome-associated quality control. *Nat. Commun.*, **8**, 159.
55. Letzring, D.P., Dean, K.M. and Grayhack, E.J. (2010) Control of translation efficiency in yeast by codon-anticodon interactions. *RNA*, **16**, 2516–2528.
56. Tesina, P., Lessen, L.N., Buschauer, R., Cheng, J., Wu, C.C., Berninghausen, O., Buskirk, A.R., Becker, T., Beckmann, R. and Green, R. (2020) Molecular mechanism of translational stalling by inhibitory codon combinations and poly(A) tracts. *EMBO J.*, **39**, e103365.